

Fields MITACS Undergraduate Summer Research Program

EEG Inverse Problem

by

Bilal Abbasi, Carrie Bragnalo, Feng Chi, Jiho Han and Iryna Sivak

Supervisors:

Nicholas Hoell and Adrian Nachman

Abstract

This project aims to understand the EEG source localization medical imaging problem. One main approach taken was to understand a solution to the inverse problem called eLORETA and see if any improvements can be made to this algorithm. An alternate approach to the problem using variational methods was also explored.

Acknowledgements

We would like to thank MITACS and the Fields Institute for making this opportunity available to us this summer. This program has equipped us with some invaluable tools that will most certainly help us in our future mathematical endeavours. Thank you also to Dr. Mark Doidge and Mario Garingo for giving their time to help us better understand the problem at hand, for emphasizing the significance of this research and for training us on their brain imaging software Dynamic Electrical Cortical Imaging (DECI). Finally we would like to thank Nicholas Hoell and Adrian Nachman for giving of their time to supervise this project and give us guidance on our way.

Contents

Abstract	i
Acknowledgements	ii
Introduction	1
1. Overview of the Project	1
2. Biological Background	1
3. eLORETA	3
Chapter 1. eLORETA algorithm	5
Chapter 2. Adjoint Method	7
1. Motivation	7
2. Approach	7
3. Solving the Forward EEG Problem via the Boundary Element Method	9
4. Application of Adjoint Method to EEG Inverse Problem	9
Chapter 3. Dynamic Electrical Cortical Imaging	11
Bibliography	14

Introduction

1. Overview of the Project

Electroencephalography (EEG) is a non-invasive means by which electrical brain activity can be measured. By placing electrodes on the scalp of a patient, the EEG measures the electric scalp potential differences which are produced by neurons firing in different regions of the brain. The EEG neuroimaging problem consists of a forward problem and an inverse problem. For a given a source current in the brain the forward problem, which is considered well posed, simulates the field distribution on the head surface by calculating the lead field. The inverse problem involves reconstruction of the primary source currents by localizing the electrical activity in the cortex from the EEG measurements. The biggest challenge that the inverse problem poses to mathematicians is that it is ill-posed since the solution is not unique and is not stable. There are infinitely many possible source configurations that could result from a given EEG since the relationship between current sources and the electromagnetic field is not one-to-one. The system to be solved is also severely ill-conditioned meaning that there are many more unknowns than equations to be solved. [1] It is up to mathematicians to decide which source configuration is the most accurate given the EEG data.

In order to study the inverse problem of the EEG it is almost always necessary to use the lead field, which relates brain sources to the retrieved measurements, as an input. As a group we took two different approaches to the problem. A solution to the inverse problem which uses the algorithm called eLORETA uses a Bayesian statistical approach. Half of the group looked at this algorithm with the goals of understanding how it works and determining if it is a viable solution. We believe that there may be some downfalls to eLORETA as a viable solution to the inverse problem due to assumptions which this method makes. The other half of the group approached the problem from the variational side by studying the adjoint method of solving the problem, which begins with Maxwell's equations.

2. Biological Background

In order to better understand the EEG inverse problem it helps to understand what is happening on the biological level. The fundamental building block of the nervous system in humans is the neuron. The structure of the neuron is shown in Figure 1. As in all

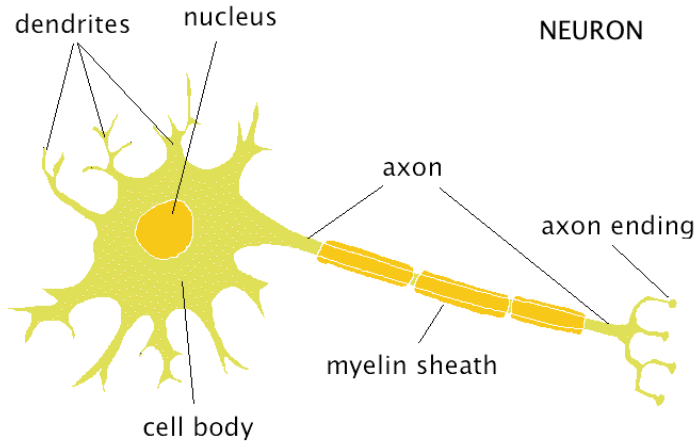


FIGURE 1. Structure of the neuron. [4]

other cells in the body, the cell body in neurons contains the genetic information as well as infrastructure to carry out basic metabolism of the cell. What separates the neuron from other types of cells is the presence of dendrites and an axon. The dendrite is a place where the neuron integrates input from other neurons, which can be either excitatory or inhibitory. When a certain threshold of inputs is met, the axon is the region where the action potential is propagated. Then, a specific neurotransmitter is released at the end of the axon through a process called a synapse.

The released neurotransmitters from the synapse bind to receptors present in dendrites of another neuron which leads to a postsynaptic potential (PSP). It is known that electrical potential differences in the scalp are caused by these PSPs [3]. There are two types of PSPs: IPSP (inhibitory) and EPSP (excitatory). IPSPs causes the postsynaptic neuron to depolarize (voltage is less negative) whereas EPSPs causes hyperpolarization (voltage is more negative). If a certain number of EPSP signals are received, the voltage reaches a threshold, which causes the postsynaptic neuron to release its own neurotransmitters. The scalp electrical potential is determined by the spatial summation of the current density from PSPs that occur synchronously in a cluster of neurons [3]. Although all neurons contribute to the EEG signals, EEG signals are primarily generated by neurons in the cortical surface (cortical pyramidal neurons) that are oriented perpendicular to the surface [3]. Moreover, one active neuron is not enough to generate a measurable EEG signal. Only when cortical pyramidal neurons are arranged in parallel and synchronized can the EEG detect the signal [3].

The neural activity can be physically modeled by current dipoles. When neurotransmitters are released in a synapse, they bind to receptors of the postsynaptic neuron. In the case of EPSP, this usually causes an influx of Na^+ (positive) ions. This causes a sink to be created, resulting in a more negative charge on the basal side. The source of the current is located at the apical region, where there is an influx of negative ions and an outflow of positive ions. In summary, this generates a current dipole and this model is shown in Figure 2.

3. eLORETA

The currently accepted solution to the inverse EEG problem is exact low resolution brain electromagnetic tomography (eLORETA). eLORETA is claimed to be a genuine solution which has zero error and no localization bias. At first glance it seems to be a perfect solution to the problem and that nothing can be done to enhance it. According to Dr. Mark Doidge, who is the impetus for the project, "this is the algorithm to beat". As we dig into the details of the algorithm, however, eLORETA is only perfect under ideal conditions and assumptions. Roberto D. Pascual-Marqui, who developed the eLORETA algorithm, states in [3] that eLORETA is proved to have no localization error when there is only one source or a few uncorrelated sources. Both of these conditions do not seem to be very practical. Based on the discussions we had with Dr. Doidge it seems that multiple sources are often correlated. These problems have not gone unnoticed and at the end of Chapter 5 of [3] Pascual-Marqui mentions new approaches to the problem using Bayesian formulation which opens the door to the consideration of more complicated and realistic conditions. Throughout the summer we read a variety of papers outlining various

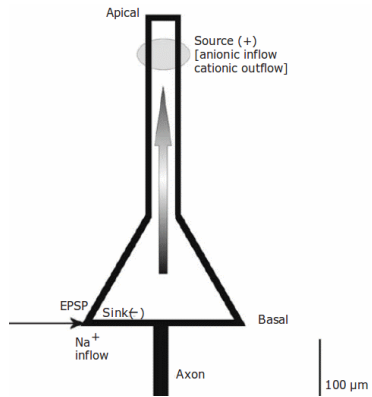


FIGURE 2. Current dipole in a neuron, which is the building block of EEG signals. [3]

approaches, including Bayesian approaches and hierarchical Bayesian approaches, which aimed to resolve some of the current downfalls of eLORETA.

CHAPTER 1

eLORETA algorithm

Consider the forward EEG equation:

$$\phi = KJ + c\bar{1},$$

where $\phi \in \mathbb{R}^{N_E}$ – scalp electric potential differences, measured at N_E electrodes with respect to a single reference electrode where $K = (K_1, K_2, \dots, K_{N_V}) \in \mathbb{R}^{N_E \times (3N_V)}$ is the lead field matrix corresponding to N_V voxels, $J \in \mathbb{R}^{(3N_V)}$ is the current density and c is a scalar accounting for the physics nature of electric potentials which are determined up to constant, $\bar{1} = (1, \dots, 1) \in \mathbb{R}^{N_E}$.

Estimating c from minimization problem

$$\hat{c} = \min_c \|\Phi - KJ - c\bar{1}\|^2,$$

we obtain the solution:

$$\hat{c} = \frac{\bar{1}^T}{\bar{1}^T \bar{1}} (\Phi - KJ).$$

Plugging \hat{c} into EEG equation gives

$$H\phi = HKJ$$

where $H = I - \frac{\bar{1}\bar{1}^T}{\bar{1}^T \bar{1}}$ is the average reference operator and $I \in \mathbb{R}^{N_E \times N_E}$ is identity matrix. Hereafter $\phi := H\Phi$, $K := HK$. Therefore $\phi = KJ$.

The family of solutions that attains exact, zero error localization of point-test sources anywhere in the brain can be parameterized by a symmetric matrix $C \in \mathbb{R}^{N_E \times N_E}$ such that

$$\hat{j}_i = [(K_i^T C K_i) K_i^T C] \phi.$$

Here $J = (j_1, j_2, \dots, j_{N_E})^T$, $j_i \in \mathbb{R}^3$, denotes the current density at the i -th voxel.

eLORETA is based on the regularized, weighted minimum norm problem:

$$\min_J \|\phi - KJ\|_2^2 + \alpha J^T W J.$$

Here $W \in \mathbb{R}^{(3N_V) \times (3N_V)}$ is a given symmetric weight matrix and $\alpha \geq 0$ is regularization parameter. The solution is linear

$$\hat{J} = T\phi$$

with

$$T = W^{-1} K (K W^{-1} K^T + \alpha H)^+.$$

Hereafter the superscript “+” denotes the Moore-Penrose pseudoinverse.

One can obtain the same minimization problem from the Bayesian point of view. We have measurements of electric potentials on the scalp:

$$\phi = KJ + \varepsilon,$$

with normally distributed noise in measurements $\varepsilon \sim \mathcal{N}(0, \alpha H)$, $J \sim \mathcal{N}(0, \Sigma_J)$ with the “a priori” covariance matrix $\Sigma_J = W^{-1}$.

Maximization of loglikelihood function leads to the same weighted minimum norm problem:

$$-\log p_{post}(J|\Phi) \propto \|\Phi - KJ\|_2^2 + \alpha J^T \Sigma^{-1} J = \|\Phi - KJ\|_2^2 + \alpha J^T W J \rightarrow \min_J.$$

Based on the linear relation of the solution $\hat{J} = T\Phi$ we can obtain the explicit form of the a posteriori covariance matrix for the estimated current density:

$$\Sigma_{\hat{J}} = W^{-1} K^T (K W^{-1} K^T + \alpha H)^+ K W^{-1}.$$

If $W = \text{diag}(W_1, \dots, W_{N_v})$ with blocks $W_j \in \mathbb{R}^{3 \times 3}$, $j = 1, \dots, N_v$, then the solution to the problem

$$\widehat{W} = \underset{W}{\text{argmin}} \|I - \Sigma_{\hat{J}}\| = \underset{W}{\text{argmin}} \|I - W^{-1} K^T (K W^{-1} K^T + \alpha H)^+ K W^{-1}\|$$

produces an inverse solution with zero error localization of point-source electrical signal.

This solution satisfies following set of matrix equations:

$$\widehat{W}_j^2 = K_j^T (K \widehat{W}^{-1} K^T + \alpha H)^+ K_j$$

for all $j = 1, \dots, N_v$.

Thus the following iterative algorithm converges to the block-diagonal weights W :

Input: lead field K , regularization parameter $\alpha \geq 0$.

Initialize weight matrix $W = I$.

Repeat until convergence:

- $M := (K W^{-1} K^T + \alpha H)^+$
- For $j = 1, \dots, N_v$:

$$W_j = [K_j^T M K_j]^{SymmSqrt},$$

SymmSqrt denotes the symmetric square root

Output: \widehat{W} .

Finally, estimation of weight matrix \widehat{W} obtained from the algorithm provides the eLORETA inverse solution

$$\hat{J} = \widehat{W}^{-1} K (\widehat{W}^{-1} K^T + \alpha H)^+ \phi.$$

CHAPTER 2

Adjoint Method

1. Motivation

Rather than simple look at the problem from an approach that has widely been studied, we decided to also take a road less travelled and study the inverse problem from the variational side beginning with Maxwell's equations. The adjoint method provides a simpler way of calculating the lead field for a given measurement than method previously proposed.

2. Approach

The Adjoint State approach is a variational approach which mainly consists of examining functionals which are defined over Hilbert Spaces. Consider a real Hilbert space W on an open bounded region Ω with inner product $\langle u, v \rangle$ and \mathbf{p} a set of parameters in some functional space W_3 . The for some $\forall \mathbf{p} \in W_3$ and $v \in W$, the state equation is:

$$(2.1) \quad \mathbf{A}(\mathbf{p})v(\mathbf{p}) = f(\mathbf{p})$$

where $\mathbf{A}(\mathbf{p}) : W \rightarrow W_1 \subset W$ is a linear operator and $f = f(\mathbf{p})$ is a function on W_1 .

We can rewrite 2.1 using an arbitrary test function $w \in W_2$:

$$(2.2) \quad \langle \mathbf{A}(\mathbf{p})v(\mathbf{p}) - f(\mathbf{p}), w \rangle = 0$$

If $v = v(\mathbf{p})$ satisfies 2.2 we call v a state function. We assume measurements taken can be modeled as the application of a linear operator, $\mathbf{M}(\mathbf{p}) : W \rightarrow \mathbb{R}$, to our state functions v . We then define the error functional $\mathcal{J}(\mathbf{p})$, with m as our observed measurements

$$(2.3) \quad \mathcal{J}(\mathbf{p}) = \frac{1}{2} \|\mathbf{M}(\mathbf{p})v(\mathbf{p}) - m\|^2$$

where $\|\cdot\|$ is the standard Euclidean norm.

Our inverse problem is then to find a \mathbf{p} which minimizes 2.3 which we subject to condition 2.2 holding. Therefore our minimization problem can be formally stated as:

$$(2.4) \quad \min_{\mathbf{p} \in W_3} \mathcal{L}(v, w; \mathbf{p}) = \min_{\mathbf{p} \in W_3} (\mathcal{J}(\mathbf{p}) + \langle w, \mathbf{A}(\mathbf{p})v(\mathbf{p}) - f(\mathbf{p}) \rangle)$$

where w can be thought of as a Lagrange multiplier. Recall that the Lagrangian \mathcal{L} is a functional from the cartesian product $W \times W_2 \times W_3$ into \mathbb{R} and is assumed to be differentiable. The differentiability of \mathcal{L} allows us to define the Gateaux derivative of \mathcal{L} . For a definition of a Gateaux differentiable function, refer to Definition 1 of [1].

If v satisfies 2.2, then \mathcal{L} becomes:

$$(2.5) \quad \mathcal{J}(\mathbf{p}) = \mathcal{L}(v(\mathbf{p}), w; \mathbf{p}).$$

With this v , we now take the Gateaux derivative of both sides of 2.4 with respect to \mathbf{p} :

$$(2.6) \quad \delta\mathcal{J} = \frac{d}{dt}|_{t=0}\mathcal{J}(\mathbf{p} + t\phi) = \frac{d}{dt}|_{t=0}\mathcal{L}(v(\mathbf{p} + t\phi), w; \mathbf{p} + t\phi)$$

$$(2.7) \quad = \frac{\partial\mathcal{L}}{\partial v}\delta v + \frac{\partial\mathcal{L}}{\partial\mathbf{p}}\delta\mathbf{p}$$

We now require that the first term in 2.7 be equal to zero:

$$(2.8) \quad \frac{\partial\mathcal{L}}{\partial v}(v, w; \mathbf{p})\delta v = 0 \quad \forall\delta v$$

Expanding this we get

$$(2.9) \quad \langle \mathbf{M}(\mathbf{p})v(\mathbf{p}) - m, \mathbf{M}(\mathbf{p})\delta v \rangle + \langle w, \mathbf{A}(\mathbf{p})\delta v \rangle = 0 \quad \forall\delta v.$$

Since our inner product is defined on a Hilbert space we have that for any linear operator \mathbf{H} : $\langle x, \mathbf{H}y \rangle = \langle \mathbf{H}^*x, y \rangle$, where \mathbf{H}^* denotes the **adjoint** of \mathbf{H} . This notion comes from defining a continuous linear functional $g(y) : H \rightarrow \mathbb{R}$, where $g(y) = \langle x, \mathbf{B}y \rangle$, $x \in H$ and \mathbf{B} is a linear operator. Using the Riesz Representation Theorem, we know $\exists!z \in H$ s.t. $g(y) = \langle x, \mathbf{B}y \rangle = \langle z, y \rangle \forall y \in H$. [1] z is defined to be \mathbf{B}^*x . Since both \mathbf{M} and \mathbf{A} are linear operators, 2.8 is equivalent to

$$(2.10) \quad \langle \mathbf{M}^*(\mathbf{p})(\mathbf{M}(\mathbf{p})v(\mathbf{p}) - m), \delta v \rangle + \langle \mathbf{A}^*(\mathbf{p})w, \delta v \rangle = 0 \quad \forall\delta v$$

$$(2.11) \quad \Leftrightarrow \langle \mathbf{M}^*(\mathbf{p})(\mathbf{M}(\mathbf{p})v(\mathbf{p}) - m) + \mathbf{A}^*(\mathbf{p})w, \delta v \rangle = 0 \quad \forall\delta v$$

$$(2.12) \quad \Leftrightarrow \mathbf{M}^*(\mathbf{p})(\mathbf{M}(\mathbf{p})v(\mathbf{p}) - m) + \mathbf{A}^*(\mathbf{p})w = 0$$

and clearly 2.8 \Leftrightarrow 2.12. We call this last expression the adjoint state equation and w the adjoint state function. Therefore given that v satisfies 2.1 and w satisfies 2.12, the Gateaux-derivative of \mathcal{L} with respect to \mathbf{p} becomes:

$$(2.13) \quad \delta\mathcal{J}(\mathbf{p}) = \frac{\partial\mathcal{L}}{\partial\mathbf{p}}(v, w; \mathbf{p})\delta\mathbf{p}$$

Using this last expression, we can define an algorithm to find a \mathbf{p} that satisfies 2.4.

- (1) Start with an initial guess \mathbf{p}_0 . Set $i = 0$.
- (2) Solve 2.1 for v_i .
- (3) Solve 2.12 for w_i .
- (4) Use v_i, w_i, \mathbf{p}_i and calculate $\delta\mathcal{J}(\mathbf{p}_i)$.
- (5) Calculate \mathbf{p}_{i+1} using $\delta\mathcal{J}(\mathbf{p}_i)$.
- (6) If $\|\mathbf{p}_i - \mathbf{p}_{i+1}\| < \text{tol}$ then STOP. Otherwise set $i = i + 1$ and start back at Step 1.

3. Solving the Forward EEG Problem via the Boundary Element Method

In attempting to solve an inverse problem, which is typically ill-posed, it can be helpful to know how to solve the forward problem first. In particular, the application of the adjoint method employs the solution of the forward problem. In the EEG problem, one way to solve the forward problem is to use the Boundary Element Method (BEM). In the BEM, we split the brain into three homogenous, isotropic conducting regions (four regions if including the outside of the head) and then use the potential on the interfaces of these regions to calculate the potential anywhere in the brain. Furthermore, each of these interfaces are tessellated into triangles and an approximation of V on an interface S_j is given as $V(\mathbf{r})|_{S_j} \approx \tilde{V}^j(\mathbf{r}) = \sum_{i=1}^{N_j} V_i^j h_i^j(\mathbf{r})$. This is expressed by the following equation:

$$(3.1) \quad V(\mathbf{r}) = \frac{2\sigma_0}{\sigma_k^- + \sigma_k^+} V_0(\mathbf{r}) + \frac{1}{2\pi} \sum_{j=1}^3 \frac{\sigma_j^- - \sigma_j^+}{\sigma_k^- + \sigma_k^+} \sum_{k=1}^{N_j} \sum_{i=1}^{N_j} V_i^j \int_{\mathbf{r}' \in \Delta S_{j,k}} h_i^j(\mathbf{r}') \frac{\mathbf{r}' - \mathbf{r}}{\|\mathbf{r}' - \mathbf{r}\|^3} dS_j$$

where

S_j - Interface between region Ω_j and Ω_{j+1} .

$V_0(\mathbf{r})$ - Potential at \mathbf{r} for an infinite medium with conductivity σ_0 .

σ_k - Conductivity of medium for which \mathbf{r} is in.

σ_j^- , σ_j^+ - Conductivities of the inner and outer compartments divided by the interface S_j , respectively.

$\Delta S_{j,k}$ - k th triangle in the tessellation of S_j .

V_i^j - Coefficients are unknown on S_j and are determined by constraining to $\tilde{V}^j(\mathbf{r})$ satisfy (19) at certain points, known as collocation points.

Numerically, this can be represented by a linear system

$$(3.2) \quad \mathbf{V} = \mathbf{BV} + \mathbf{V}_0$$

where

\mathbf{V} - Column vectors denoting at every node the unknown potential due to a source.

\mathbf{V}_0 - Column vectors denoting potential value in an infinite homogeneous medium.

\mathbf{B} - Matrix generated from the integrals, that depend on the geometry of the interfaces and the conductivities of each region.

Thus the BEM is reduced to a linear system.

4. Application of Adjoint Method to EEG Inverse Problem

In the EEG problem, we select our $W = L^2(\Omega)$, where Ω is largely the brain or homogeneous region of it.

The data given is supposed to be modeled by the difference of potentials at some locations $\mathbf{r}_1, \dots, \mathbf{r}_{n_V}$ on the scalp and a reference \mathbf{r}_0 . Let v_1, \dots, v_{n_V} be the measured data, where n_V represents the number of distinct electrodes.

We would like to obtain a \mathbf{J}^p that best replicates the given data. Let $V = V(\mathbf{J}^p(\mathbf{r})) = V(\mathbf{r})$ denote the electric potential at position \mathbf{r} . From the quasi-static Maxwell's Equations we have that $V(\mathbf{r})$ must satisfy the first condition in 4.1, and we impose the additional boundary condition:

$$(4.1) \quad \begin{cases} \nabla \cdot (\sigma \nabla V(\mathbf{r})) = \nabla \cdot \mathbf{J}^p & \text{in } \Omega \\ \frac{\partial V}{\partial \mathbf{n}} = \nabla V \cdot \mathbf{n} = g & \text{on } S = \partial \Omega \end{cases}$$

We also assume that the primary current source is located within the brain, and so $\mathbf{J}^p|_S = 0$. We would like to obtain a \mathbf{J}^p which minimizes:

$$\mathcal{J}_V = \frac{1}{2} \sum_{i=1}^{n_V} (V(\mathbf{r}_i) - V(\mathbf{r}_0) - v_i)^2$$

Labelling V to be our state function and 4.1 to be it's corresponding state equation we get our functional, which we would like to minimize, as

$$(4.2) \quad \mathcal{L}_V = \mathcal{L}_V(V, w; \underbrace{\sigma, \mathbf{J}^p}_{\mathbf{p}}) = \frac{1}{2} \sum_{i=1}^{n_V} (V(\mathbf{r}_i) - V(\mathbf{r}_0) - v_i)^2 + \langle \nabla \cdot (\sigma \nabla V(\mathbf{r})) - \nabla \cdot \mathbf{J}^p, w \rangle$$

And it's subsequent adjoint state function is

$$(4.3) \quad \begin{cases} \sum_i ((V(\mathbf{r}_i) - V(\mathbf{r}_0) - v_i)(\delta(\mathbf{r} - \mathbf{r}_i) - \delta(\mathbf{r} - \mathbf{r}_0))) = 0 & \text{in } \Omega \\ \nabla w \cdot \mathbf{n} = 0 & \text{on } \partial \Omega \end{cases}$$

We will assume that σ is known. And so when w and V satisfy their respective equations, the Gateaux-derivative of our functional with respect to \mathbf{J}^p becomes (with test function $\phi(\mathbf{r}) \in L(\Omega)$)

$$(4.4) \quad \delta \mathcal{L}_V = \frac{\partial \mathcal{L}}{\partial \mathbf{p}} = \frac{\partial \mathcal{L}}{\partial \mathbf{J}^p} = \int_{\Omega} \nabla w \cdot \phi(\mathbf{r}) d\mathbf{r}$$

Using Riesz Representation theorem, 4.4 tells us that the gradient of \mathcal{L} with respect to \mathbf{J}^p is then

$$(4.5) \quad \text{grad} \mathcal{L}_V(\mathbf{J}^p) = \nabla w$$

We can use this definition of the gradient in the aforementioned algorithm to obtain a suitable \mathbf{J}^p .

CHAPTER 3

Dynamic Electrical Cortical Imaging

Dynamic Electrical Cortical Imaging (DECI) is a software developed by Cerebral Diagnostics Canada that allows to generate 3D brain movies in near real time based on EEG signals. DECI implements the algorithm used in eLORETA. The figures shown below are EEG signals (right) and the corresponding the 3D brain images (left). In the 3D images, the blue arrows represent the head whereas the red arrows represent the tail of the dipole vector. The images of the brain are from "bird's eye" view where the z-axis is the top of the head, y-axis is the front (nose), and the x-axis is the right side (ear).

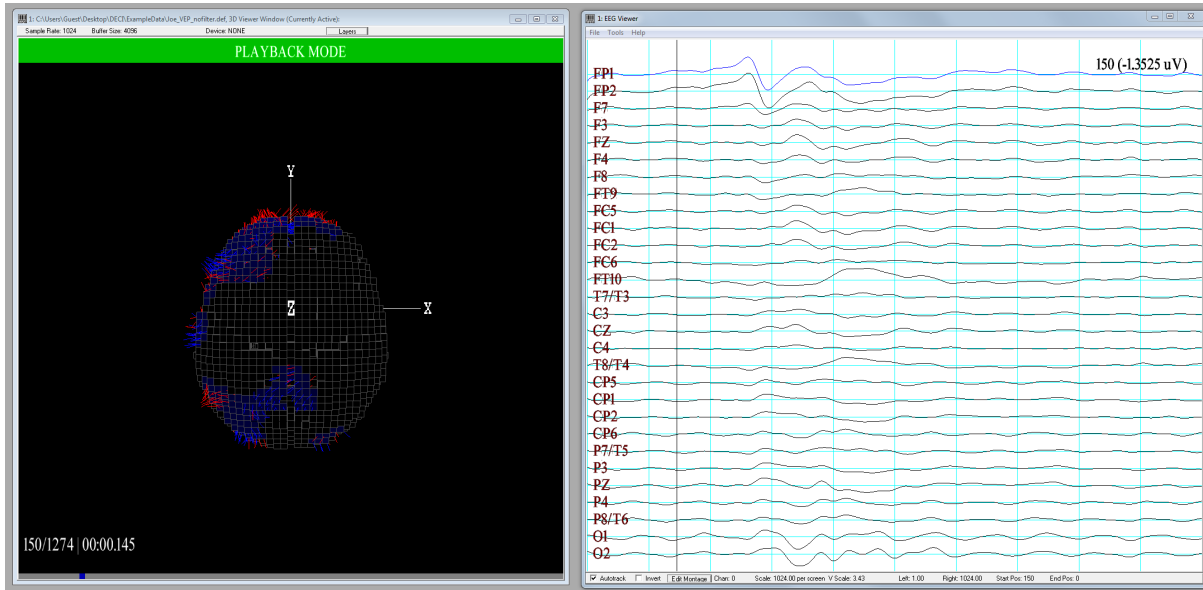


FIGURE 1. EEG signal and corresponding 3D brain image of a subject before stimulus.

In this section, a subject was exposed to a bright light towards his eye. His brain activity was recorded using EEG and an amplifier. As a response to a visual stimulus, it is expected to observe activity in the occipital lobe which contains the primary visual cortex. The vertical bar shows the time when the 3D image was taken.

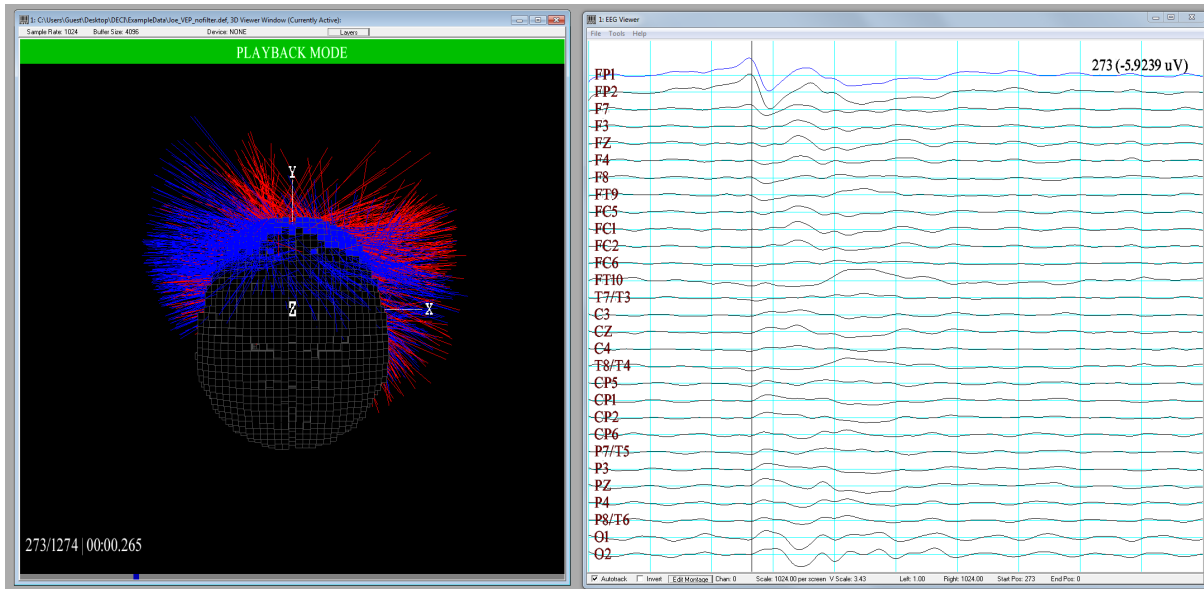


FIGURE 2. EEG of the brain response of a subject upon exposure to bright light.

In the EEG data, the electrodes labeled as "FP1" and "FP2" (refer to Figure 4 for the locations of the electrodes) show a distinct peak at the moment when the 3D image was generated.

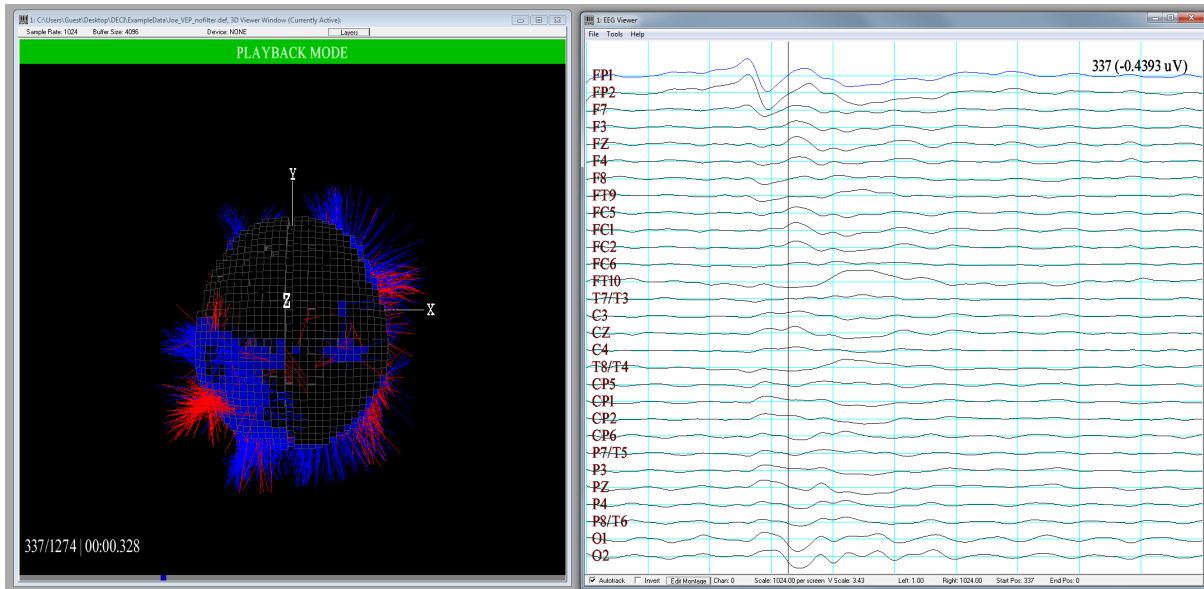


FIGURE 3. A screenshot of the EEG showing when the occipital lobe is activated.

The electrodes are placed on the skull according to the International 10-20 System, which is widely used and accepted for electroencephalography. The names of the electrode locations are based on the region of the skull in which they are found. For example the electrode FP1 is found in the frontal parietal region on the left side of the head, from the subject's point of view. The electrode O2 is found at the occipital lobe on the right side of the head and CZ is found in the central part along the midline of the skull, which connects the nasion to the inion. The five regions in which electrodes are located are frontal lobe F, central C, parietal lobe P, temporal lobe T, and occipital lobe O. All electrodes ending in an odd number are located on the left side of the skull, electrodes with even numbers are located on skull's right hemisphere and electrodes with the letter Z lie on the midline.

The specific placement of electrodes for each patient is determined with respect to the nasion and the inion. The nasion is the point at which the nose and the forehead intersect and the inion is found at the back of the head at the bottom of the skull. Often there is a prominent bump indicating the location of the inion. Various lines and curves are then drawn on the skull connecting these two points. Several other important points are then identified and used in drawing subsequent curves. Two curves must intersect to confirm the correct location for the placement of an electrode before this location is considered finalized. A diagram of the common electrode placements can be seen in the Figure 4 below.

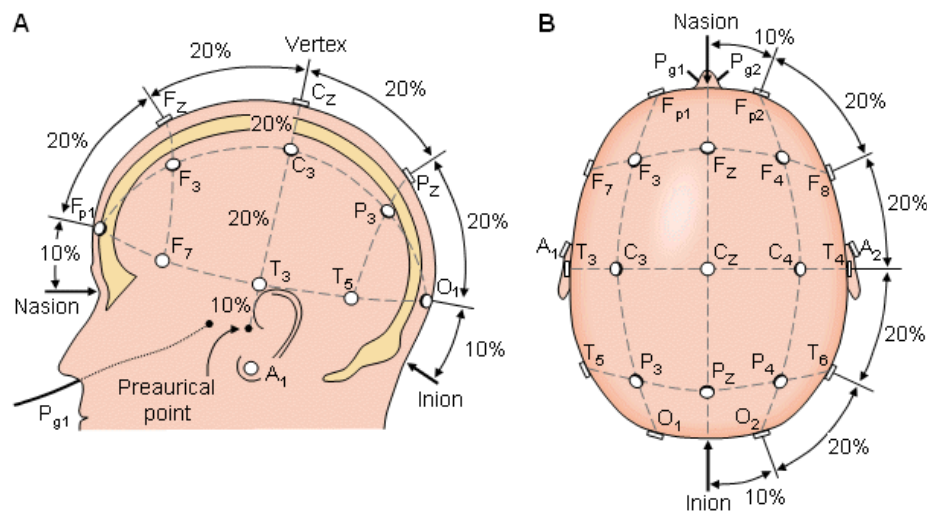


FIGURE 4. The location of electrodes on a human head based on the International 10-20 System.

Bibliography

- [1] O. Faugeras, F. Clment, R. Deriche, Dr., R. Keriven, T. Papadopoulo, J. Roberts, T. Viville, F. Devernay, J. Gomes, G. Hermosillo, P. Kornprobst, and D. Lingrand. The Inverse EEG and MEG Problems : The Adjoint State Approach I: The Continuous Case. Rapport de recherche RR-3673, INRIA, 1999. Projet CERMICS. 1, 7, 8
- [2] R. D. Pascual-Marqui. Discrete, 3D distributed, linear imaging methods of electric neuronal activity. Part 1: exact, zero error localization. ArXiv e-prints, Oct. 2007. 6
- [3] Roberto D. Pascual-Marqui: Theory of the EEG Inverse Problem, Chapter 5, pp: 121-140. In: Quantitative EEG Analysis: Methods and Clinical Applications, Eds: S. Tong and N.V. Thakor; 2009 Artech House, Boston 2, 3
- [4] <http://webspace.ship.edu/cgboer/neuron.gif> 2